RSC Advances

PAPER

View Article Online
View Journal | View Issue



Cite this: *RSC Adv.*, 2020, **10**, 32671

# Removal of reactive brilliant red X-3B by a weak magnetic field enhanced Fenton-like system with zero-valent iron†

Liping Liang,[ab] Yuting Zhang,[a] Liubiao Cheng,[a] Qian Wu,[a] Yuanyuan Xue,[a] Qian Wang[a] and Xu Meng*[cd]

The effect of a weak magnetic field (WMF) on the removal of reactive brilliant red X-3B (X-3B) by zero-valent iron (ZVI)/$H_2O_2$ was studied. The optimum conditions for the removal of X-3B by the ZVI/$H_2O_2$/WMF system were as follows: pH = 4.0, X-3B was 50 mg $L^{-1}$, $H_2O_2$ was 8 mM, and ZVI with particle size of 20 μm was 0.5 g $L^{-1}$. The X-3B decolorization rate could reach 99.41% in 10 minutes. The superposed WMF increased the working pH of ZVI from 3.0 to 4.0. The main part of ZVI/$H_2O_2$ removal kinetics of X-3B followed the zero order rate law. In this study, the removal effect of X-3B by pre-magnetization ZVI was not as good as that of real-time magnetization, but it was better than the removal of X-3B by the ZVI/$H_2O_2$ system. The ZVI/$H_2O_2$/WMF system still had the ability to remove X-3B after 4 consecutive cycles. The use of WMF improved the removal of X-3B by ZVI/$H_2O_2$ mainly due to the corrosion of ZVI. Under acidic conditions, WMF enhanced the activity of ZVI, which promoted the efficiency of the Fenton reaction. The use of WMF to enhance the ZVI/$H_2O_2$ removal X-3B was a promising and environmental friendly process because it did not require additional energy and expensive reagents and did not cause secondary pollution.

Received 18th April 2020
Accepted 23rd August 2020

DOI: 10.1039/d0ra03480k

rsc.li/rsc-advances



## Introduction

Dye wastewater from the textile, dyeing, and printing industries has been a serious environmental problem in China. Discharge wastewater from the manufacture of textiles, clothing, and apparel reached 2.0 billion tons which exceeded 10% of the total industrial wastewater in China.[1] About 2–12% of synthetic dyes were directly released into the water environment in the process of production and use. Of all dyes, azo dyes accounting for about 70% of the total synthetic dye production[2] are the most widely used dyes in the world.[3] Azo dyes with one or more azo groups (–N=N–) connected to aromatic rings exhibited an excellent water-solubility, and relative stability during usage.[4] Azo dyes not only lead to high color in water,[5] but also induced serious human and animal health problems due to their potential mutagenicity, carcinogenicity, and toxicity.[6] Besides, azo dyes in water were very stable for their commercial requirement[7] which induced their resistance to traditional biodegradation and gentle photodegradation. So it's necessary to develop new strategies to treat azo dyes in wastewater.

Common chemical treatments such as coagulation,[8] filtration,[9] adsorption,[10] and ion exchange[11] have been used to treat azo dye wastewater, but these methods have some disadvantages such as high cost, secondary pollution, low efficiency, and the inability to destroy complex structures of dyes. Compared to other chemical technologies, chemical oxidation method especially for advanced oxidation processes (AOPs) have become an excellent strategy to rapidly degrade dyes in water. Generally, AOPs requires the addition of additional energy (such as light, ultrasound, and microwave) or different catalysts into oxidants such as $H_2O_2$, persulfate (PDS), and peroxymonosulfate (PMS). ZVI was considered as a readily available, inexpensive, nontoxic and moderately strong reductant[12] which has been widely used in activating $H_2O_2$ and PDS.[13] Generally, ZVI possessed a high reactivity exhibited an excellent performance in AOPs. So, many methods have been developed to improve the reactivity of ZVI samples such as acid washing,[14] hydrogen reduction,[15] the synthesis of nano-scale ZVI (nZVI)[16] or bimetallic.[17] However, these enhancing technologies on ZVI reactivity have some barriers of high cost,[12] hard handling, and potential ecotoxicity.[18,19] Besides, the high reactivity of ZVI might also induce the formation of iron oxides or hydroxides on the surface of ZVI which inhibited the reactions between ZVI and oxidants.[20,21] Therefore, it is very important to explore an environmental friendly method which can improve the reactivity of ZVI and hinder the formation of passivation layer on the surface of ZVI.

[a]*School of Civil Engineering, Shaoxing University, Shaoxing 312000, P. R. China*
[b]*College of Life Science, Shaoxing University, Shaoxing 312000, P. R. China*
[c]*College of Textile and Garment, Shaoxing University, Shaoxing 312000, P. R. China. E-mail: mengxu0@163.com*
[d]*Key Laboratory of Clean Dyeing and Finishing Technology of Zhejiang Province, Shaoxing University, Shaoxing, 312000, P. R. China*

† Electronic supplementary information (ESI) available: Complete XRD and SEM data, supplementary data of WMF on ZVI/$H_2O_2$ removal of X-3B under different PH conditions. See DOI: 10.1039/d0ra03480k

Recently, WMF of low cost, easy handling, and no secondary pollution has become a new technology to improve the reactivity of ZVI which can enhance contaminants removal efficiency. Guan's group[22–27] carried out a lot of researches on heavy metals and dyes removal by microscale ZVI (mZVI) coupled with WMF. Their results indicated that WMF accelerated ferrous release from ZVI and promoted the corrosion of ZVI. Besides, WMF can also recover the reactivity of aged ZVI[22] and depassivate the passive film on ZVI samples.[25] Li *et al.*[23] proved that the magnetic gradient force was the major driving force for the enhancing effect of WMF by driving the paramagnetic $Fe^{2+}$ to the place with higher MF flux intensity with magnetic lines. The movement of the paramagnetic $Fe^{2+}$ could expose more reactive sites on the ZVI samples. These advantages of enhancing ZVI reactivity induced by WMF might be also applied in AOPs. Xiong *et al.*[28,29] firstly studied various organics removal performances in ZVI/$H_2O_2$/WMF and ZVI/PDS/WMF systems, WMF exhibited a significant enhancement on organics removal rate by ZVI/$H_2O_2$ and ZVI/PDS, and the accelerating effect of WMF on 4-nitrophenol degradation by ZVI/$H_2O_2$/WMF was increased with the intensity of WMF from 5 mT to 20 mT. When the magnetic field intensity was greater than 20 mT, ZVI particles were easy to aggregate. Therefore, the optimum intensity of WMF was determined to be 20 mT. Then Zhou *et al.*[30–33] and Du *et al.*[13] also investigated WMF enhanced organic contaminants removal by ZVI/$H_2O_2$ and ZVI/PDS. And WMF accelerated the generation of reactive radicals by promoting the release of ferrous. Therefore, WMF could be considered as an excellent technology to enhance azo dyes removal in ZVI/$H_2O_2$ system.

In this study, a typical azo dye reactive brilliant red X-3B (X-3B) was selected as the target dye. And the optimal reaction conditions and removal kinetics of X-3B removal by ZVI/$H_2O_2$ coupled with WMF were investigated. Finally, mechanisms of X-3B removal in ZVI/$H_2O_2$/WMF systems were proposed.

## Materials and methods

### Materials

The ZVI used in the experiment was purchased from Haotian Nano Technology Co., Ltd (Shanghai). All chemicals were at the analytical level and were used without other treatment. The raw solution was prepared by dissolving the corresponding salt in the ultra-pure water produced in the Milli-Q reference water purification system.

### Batch experiments procedure

The laboratory-scale experimental device used in this experiment was shown in Fig. S1 (in the ESI).† The non-uniform weak magnetic field in this experiment was generated by two permanent magnets. The experiment was carried out in A (with WMF) exposed to air (as shown in Fig. S1A†). During the experiment, the permanent magnet was always placed at the bottom of the reactor and it was determined that the maximum magnetic field strength was 20 mT. This experimental method was called "real-time magnetization". The solution was mixed by continuous mechanical stirring at 400 rpm to uniformly disperse ZVI particles in the solution. At this stirring intensity, the aggregation of ZVI caused by WMF could be avoided. All experiments were carried out at 25 °C which controlled by a cryostat. A certain amount of ZVI and $H_2O_2$ were added into a reactor to initial experiments. The specific experimental conditions were: pH = 4.0, $H_2O_2$ was 8 mM, X-3B was 50 mg $L^{-1}$. Before all experiments, NaOH and HCl were be used to adjust the pH of solution. At a fixed time-interval, 5 mL of water sample was taken with a syringe, filtered through a 0.45 μm filter. The ZVI samples after reactions were collected by filtering through the 0.45 μm membrane, then washed with distilled water and freeze-dried. The pre-magnetization meant to place 0.5 g $L^{-1}$ ZVI on permanent magnet, magnetize it for different time (0.5, 1, 3, 5, 7, 10 min), immediately added it to B (without WMF) for experiment (as shown in Fig. S1B†).

### Chemical analysis

X-3B was determined at 538 nm by using a spectrophotometer (UV 752N, JinShiSu). ZVI samples were characterized by X-ray diffraction (XRD) (X'Pert Powder, Malvern Panalytical) and scanning electron microscope (SEM) (JSM-6360LV, JEOL).

## Results and discussion

### Effect of WMF on the removal of X-3B by ZVI/$H_2O_2$ at different pH

The effect of WMF on ZVI removal X-3B at pH 4.0 was shown in Fig. S2 (in the ESI),† 10.79% and 3.28% of X-3B were removed by ZVI in 60 min in the presence and absence of WMF, respectively. WMF could slightly increase the removal rate of X-3B by ZVI. The effect of WMF on the removal of X-3B by ZVI/$H_2O_2$ in the range of pH 3.0–5.0 was investigated. As shown in Fig. 1, in the absence of WMF, 93.2%, 24.6%, and 1.3% of X-3B were removed by the ZVI/$H_2O_2$ system in 20 min at pH 3.0, 4.0, and 5.0, respectively. With the increase of pH from 3.0 to 5.0, the removal rate of X-3B was significantly inhibited. Obviously, ZVI/

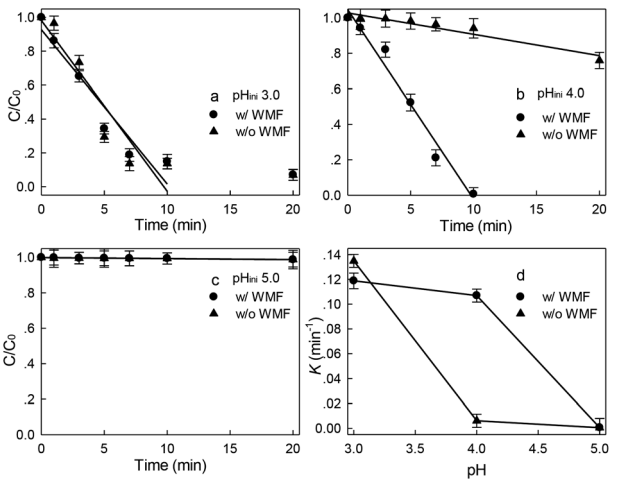


Fig. 1 Effect of WMF on ZVI/$H_2O_2$ removal of X-3B under different initial pH reaction conditions (8 mM $H_2O_2$, 50 mg $L^{-1}$ X-3B, 0.5 g $L^{-1}$ $Fe^0$, and $T$ = 25 °C).

 

$H_2O_2$ system removal of X-3B was strongly dependent on pH,[34] it was probably due to the corrosion of ZVI under strong acidic conditions (eqn (1)) (at pH 3.0), which produced more $Fe^{2+}$. But with the increase of pH from 3.0 to 5.0, the removal rate of X-3B was significantly inhibited. Only 1.3% of X-3B was observed to be degraded by ZVI/$H_2O_2$ at pH 5.0. The XRD pattern of ZVI samples was shown in Fig. S3 (in the ESI),† and no lepidocrocite was found in ZVI samples at pH 5.0. In the presence of WMF, the removal rate of X-3B at pH 3.0 did not increase. After the reaction, the ZVI samples in the ZVI/$H_2O_2$ and ZVI/$H_2O_2$/WMF systems showed abundant lepidocrocite at pH 3.0, indicating that WMF under strong acidic conditions did not enhance the reactivity of ZVI. However, about 99.4% X-3B was removed within 10 min at pH 4.0 which was much higher than that without WMF (only about 10% in 10 min), the corrosion degree of ZVI was also greatly improved, and abundant lepidocrocite were found in ZVI samples. SEM images of ZVI removal of X-3B under different pH conditions (as shown in Fig. S4†) showed that the corrosion degree of ZVI with WMF was higher than that of ZVI without WMF. Generally, X-3B degradation in ZVI/$H_2O_2$ system depended on the generation of ·OH *via* eqn (2) and (3). In a ZVI/$H_2O_2$ reaction, the release rate of $Fe^{2+}$ from ZVI particles (eqn (1) and (2)) determined the production of ·OH. Other researchers[23,26] reported that WMF accelerated the release rate of $Fe^{2+}$. So WMF could enhance X-3B removal by ZVI/$H_2O_2$. But the removal of X-3B by ZVI/$H_2O_2$/WMF was inhibited at pH 5.0. Although the corrosion of ZVI was depended on pH, Liang *et al.*[24] proved that WMF could enhance the release rate of $Fe^{2+}$ during the reduction of Se(IV) to Se(0) by ZVI at the range of 4.0–7.0. So WMF could enhance the release of $Fe^{2+}$ from ZVI at pH 5.0. But WMF did not exhibit any enhancement of X-3B removal at pH 5.0 which might be ascribed to the limitation of Fenton reactions depending on the narrow effective pH range (2.5–3.0).[35] But WMF could still extend the effective reaction pH from 3.0 to 4.0 in ZVI/$H_2O_2$ system. In addition, ZVI/$H_2O_2$ could remove neglected X-3B in 60 min at pH 4.0 in the presence of WMF (data shown in Fig. S5†). So, the removal of X-3B was ascribed to ·OH generated by eqn (3).

$$Fe^0 + 2H^+ \rightarrow Fe^{2+} + H_2 \quad (1)$$

$$Fe^0 + H_2O_2 \rightarrow Fe^{2+} + 2OH^- \quad (2)$$

$$Fe^{2+} + H_2O_2 \rightarrow Fe^{3+} + 2{\cdot}OH \quad (3)$$

Most studies[13,28] reported that contaminants removal by AOPs based on ZVI follows pseudo first-order kinetics. However, the pseudo first-order kinetics could not well simulate the main stages of X-3B removal. The zero-order kinetic model was used to describe the main part of each data set in the initial rapid removal phase, and the removal rate of X-3B by ZVI/$H_2O_2$ within 10 min in the pH range of 3.0–5.0 was described, as shown by eqn (4).

$$C_0 - C_t \rightarrow -kt \quad (4)$$

where $k$ is the X-3B zero-order rate constant ($min^{-1}$), $C_0$ is the initial X-3B concentration, and $C_t$ is the X-3B concentration at the fixed time. The fitting results were shown in Fig. 1(d). WMF increased the reaction rate constant of X-3B decolorization by 17.8 times at pH 4.0, and WMF exhibited a strong enhancement to X-3B removal at pH 4.0 in ZVI/$H_2O_2$ systems.

### Effects of initial ZVI dosages on the removal of X-3B by ZVI/$H_2O_2$ and ZVI/$H_2O_2$/WMF

Effects of ZVI dosages on X-3B removal rate by ZVI/$H_2O_2$ system were investigated with the initial X-3B concentration of 50 mg $L^{-1}$ at pH 4.0 in the presence of WMF. As shown in Fig. 2, the removal rate of X-3B was increased with the increased of ZVI dosages in the absence of WMF. Only 4.5% X-3B was removed by $H_2O_2$ coupled with 0.25 g $L^{-1}$ ZVI in 20 min. When the ZVI dosage increased to 0.5 and 1.0 g $L^{-1}$, about 24.1% and 95.1% X-3B were removed during 20 min, respectively. In the presence of WMF, the removal rate of X-3B increased at first and then decreased with the increase of ZVI dosage. About 50.0 mg $L^{-1}$ X-3B was completely removed by ZVI/$H_2O_2$/WMF at 0.5 g $L^{-1}$ ZVI in 10 min. The Lorentz force generated by WMF and the magnetic field gradient force generated by the induced magnetic field generated on the surface of ZVI promoted the corrosion of ZVI and generated more $Fe^{2+}$,[23] which promoted the Fenton system to degraded the dye. However, with the increase of ZVI dosages from 0.5 to 1.0 g $L^{-1}$, the removal rate of X-3B was seriously inhibited, it might be due to the excessive amount of ZVI that consumed the ·OH in the solution. In summary, WMF could significantly increase the removal rate of X-3B at lower ZVI dosage. The promoting effect of WMF was not obvious when the ZVI dose was 0.25 g $L^{-1}$. This might be due to the limited number of active sites on the surface of ZVI, the generation of $Fe^{2+}$ by 0.25 g $L^{-1}$ ZVI was much lower, so it was

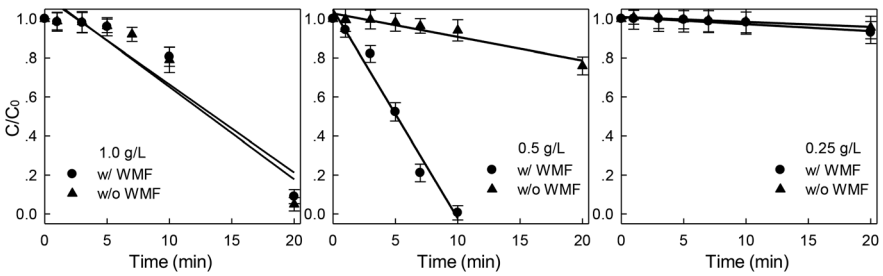


Fig. 2 Effect of WMF on ZVI/$H_2O_2$ removal of X-3B under different ZVI dosages (pH 4.0, 8 mM $H_2O_2$, 50 mg $L^{-1}$ X-3B, and $T$ = 25 °C).

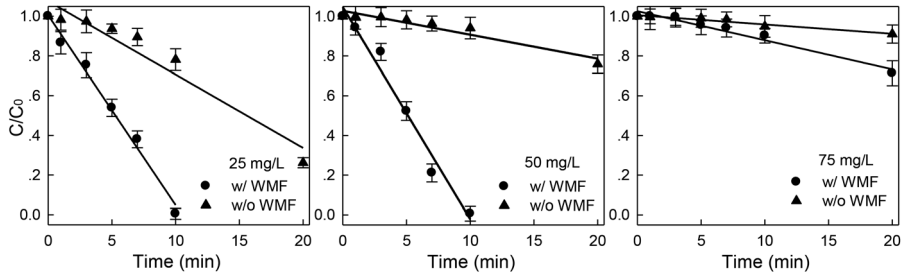


Fig. 3 Effect of WMF on ZVI/$H_2O_2$ removal of X-3B under different concentrations (pH 4.0, 8 mM $H_2O_2$, 0.5 g $L^{-1}$ $Fe^0$, and $T = 25$ °C).

Table 1 Removal kinetic constants of different X-3B concentrations

| Without WMF | | | With WMF | | |
|---|---|---|---|---|---|
| X-3B (mg $L^{-1}$) | $k_{obs}$ $min^{-1}$ | $R^2$ | X-3B (mg $L^{-1}$) | $k_{obs}$ $min^{-1}$ | $R^2$ |
| 25 | 0.037 | 0.918 | 25 | 0.108 | 0.986 |
| 50 | 0.012 | 0.903 | 50 | 0.107 | 0.971 |
| 75 | 0.005 | 0.937 | 75 | 0.015 | 0.957 |

difficult to catalyze the decomposition of $H_2O_2$ to produce more ·OH in the presence of WMF.

### Effects of initial X-3B concentrations on the removal of X-3B by ZVI/$H_2O_2$ and ZVI/$H_2O_2$/WMF

Dye concentration was another factor affecting X-3B removal rate. Fig. 3 showed the effect of WMF on X-3B removal by ZVI/$H_2O_2$ at different initial X-3B concentrations. The removal rate of X-3B by ZVI/$H_2O_2$ decreased significantly with the increase of X-3B concentration. In the presence of WMF, the removal rates reached 99.5%, 99.4% and 9.8% in 10 min at the initial X-3B concentrations of 25, 50 and 75 mg $L^{-1}$, respectively. The superimposed WMF obviously improved the removal rate of X-3B by ZVI/$H_2O_2$. Furthermore, X-3B was completely removed by ZVI/$H_2O_2$/WMF in 20 minutes in the initial X-3B concentration range of 25.0–50.0 mg $L^{-1}$. The main part of each data set in Fig. 3 could be well described by zero-order dynamics, and the fitting results were shown in Table 1. Zero-order rate constants ($k_{obs}$) were found to be in the range of 0.005–0.108 $min^{-1}$, which was significantly dependent on the initial concentration of X-3B. In the presence of WMF, $k_{obs}$ reduced linearly from 0.108 to 0.015 $min^{-1}$ with the increase of X-3B concentrations from 25.0 to 75.0 mg $L^{-1}$. This was due to non-availability of sufficient number of hydroxyl radicals. The presumed reason was that when the initial concentration of X-3B was increased, the ·OH concentration was not increased correspondingly. At the concentration of 25 mg $L^{-1}$, the generated ·OH was not exhausted. And at 75 mg $L^{-1}$, ·OH became exhausted. The application of WMF improved the removal rate of X-3B at the different initial X-3B concentrations.

### Effects of initial $H_2O_2$ concentrations on the removal of X-3B by ZVI/$H_2O_2$ and ZVI/$H_2O_2$/WMF

Effects of WMF on the removal of X-3B by ZVI at different $H_2O_2$ concentrations (4, 8, 12 mM) were investigated in Fig. 4. The removal rate of X-3B increased first and then decreased with the increase of $H_2O_2$ concentrations. More than 99.4% of X-3B could be removed when the concentration of $H_2O_2$ reached 8 mM at 10 min. But and when $H_2O_2$ concentration were 4 or 12 mM, the removal of X-3B was negligible at 20 min. This was similar to the corrosion situation of ZVI shown in Fig. S6.† Only when the $H_2O_2$ concentration was 8 mM in the presence of WMF, ZVI particles were observed to break. In other cases, the degree of ZVI corrosion was slight. The ·OH generated by $H_2O_2$ and $Fe^{2+}$ in the solution was not enough to attack the chromophores and the color-assisting groups in X-3B at a low $H_2O_2$ concentration of 4 mM. The ·OH produced by the Fenton-like reaction would react with excess $H_2O_2$ in the solution to form a weak oxidizing $HO_2^{\cdot}$, which consumed the ·OH in the solution, as shown in eqn (5). The oxidation capacity of $HO_2^{\cdot}$ was far weaker than that of ·OH, and X-3B could not be removed effectively. Besides, $Fe^{3+}$ could be reduced to $Fe^{2+}$ by excessive $H_2O_2$, which was an unfavorable reaction to remove X-3B (eqn (6) and (7)). And the optimal $H_2O_2$ concentration in this study was 8 mM.

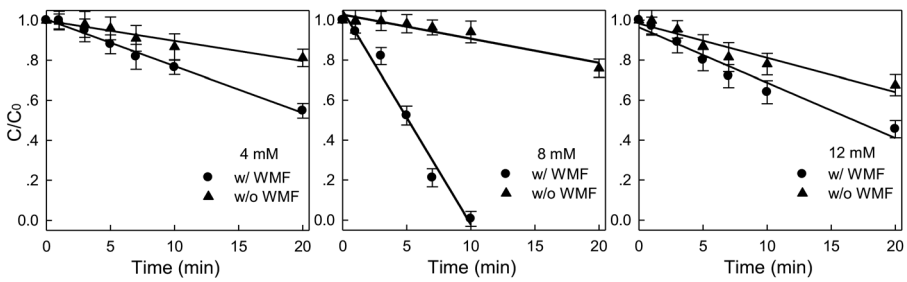


Fig. 4 Effect of WMF on ZVI/$H_2O_2$ removal of X-3B under different $H_2O_2$ concentrations (pH 4.0, 50 mg $L^{-1}$ X-3B, 0.5 g $L^{-1}$ $Fe^0$, and $T = 25$ °C).

 

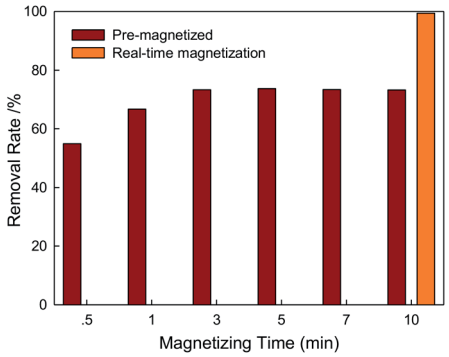


Fig. 5 Effects of magnetizing time on X-3B removal by ZVI/$H_2O_2$/WMF (pH 4.0, 8 mM $H_2O_2$, 50 mg $L^{-1}$ X-3B, 0.5 g $L^{-1}$ $Fe^0$, and $T$ = 25 °C).

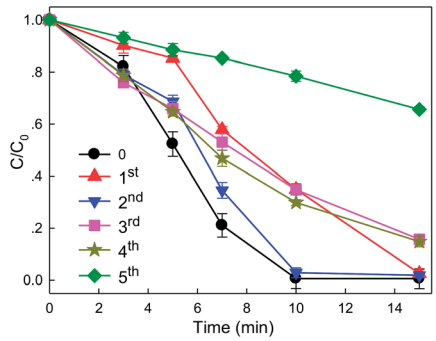


Fig. 6 Reuse efficiency of ZVI for X-3B removal by ZVI/$H_2O_2$/WMF (pH 4.0, 8 mM $H_2O_2$, 50 mg $L^{-1}$ X-3B, 0.5 g $L^{-1}$ $Fe^0$, and $T$ = 25 °C).

$$\cdot OH + H_2O_2 \rightarrow H_2O + HO_2^{\cdot} \quad (5)$$

$$Fe^{2+} + H_2O_2 \rightarrow Fe^{3+} + OH^- + \cdot OH \quad (6)$$

$$Fe^{3+} + H_2O_2 \rightarrow Fe^{2+} + HO_2^{\cdot} + H^+ \quad (7)$$

### Effects of magnetization time on X-3B removal by ZVI/$H_2O_2$/WMF

Previous experiments proved that WMF exhibited an enhancement on X-3B removal by ZVI/$H_2O_2$. Generally, ZVI possessed the magnetic memory after magnetization treatment by WMF. Herein, effects of magnetization time on X-3B were illustrated in Fig. 5. The removal rate of X-3B by ZVI/$H_2O_2$/WMF increased with the increase of magnetizing time. Without the presence of WMF, the removal rate of X-3B only reached 5.9% within 10 min. The magnetizing time of 30 s could also increase the removal rate of X-3B from 5.9% to 54.88%. So the effect of pre-magnetization ZVI removing X-3B was better than that of ZVI/$H_2O_2$ system. The removal rate of X-3B was very stable when the magnetizing time increased to 3 min. Although the WMF was discharged after the magnetizing of the solution, the removal rate of ZVI was not depressed because of the magnetic memory of ZVI. Besides, the magnetization of ZVI over the reaction time did not improve the removal rate of X-3B more. So the optimizing magnetizing time in this study was 3 min. The real-time magnetization of 10 min ZVI/$H_2O_2$/WMF system could remove 99.4% of X-3B, while the pre-magnetization of 10 min ZVI/$H_2O_2$/WMF could only remove 73.2% of X-3B. Therefore, the effect of pre-magnetization was far less than that of real-time magnetization, but this advantage of magnetic memory could shorten the magnetizing time during the reaction which was very important to the application of WMF technology by reducing magnetizing time and the reactors volume.

### Effects of ZVI reuse times on X-3B removal by ZVI/$H_2O_2$/WMF

WMF improved the reactivity of ZVI towards $H_2O_2$ by accelerating the release of ferrous. Liang *et al.*[22] found that WMF could increase the removal rate of Se(IV) by aged ZVI, and concluded that WMF induced nonuniform depassivation and eventually localized corrosion of the ZVI surface by the coeffects of the Lorentz force and the field gradient force. Then Xu *et al.*[25] also proved that the presence of WMF could restore the reactivity of the aged ZVI samples with $Fe_3O_4$, α-$Fe_2O_3$, γ-FeOOH as the passive film. So, the reusability of ZVI in the presence of WMF could also be improved. As shown in Fig. 6, the reuse experiments of ZVI for X-3B removal kinetics coupled with $H_2O_2$ was studied. The removal rate of X-3B by ZVI/$H_2O_2$/WMF was inhibited in the 1st reuse experiment especially in the initial 5 min. The generation of iron oxides on the surface of ZVI after the first run reaction limited the reaction between ZVI and $H_2O_2$. But the presence of WMF could recover the reactivity of ZVI after 5 min. And the final removal rate at 15 min reached almost 100%. And the removal rate of X-3B by ZVI/$H_2O_2$/WMF was promoted after ZVI reused 1 times, but still was lower than the initial run reaction. The removal rate of X-3B during the 2nd

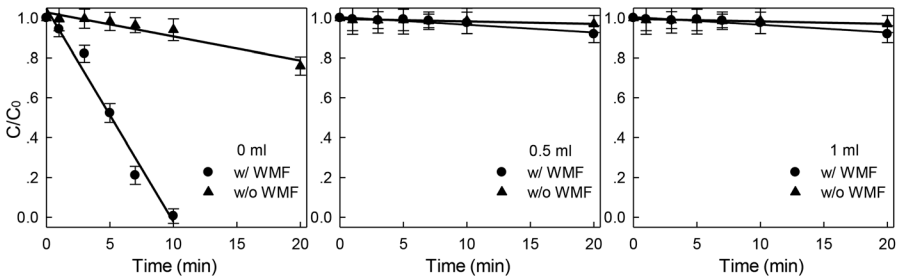


Fig. 7 Effect of WMF on ZVI/$H_2O_2$ removal of X-3B under different methanol dosages (pH 4.0, 8 mM $H_2O_2$, 50 mg $L^{-1}$ X-3B, 0.5 g $L^{-1}$ $Fe^0$, and $T$ = 25 °C).

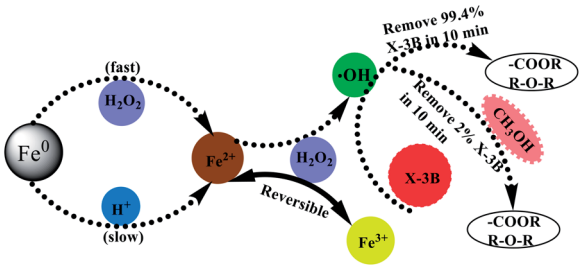


Fig. 8 Mechanism diagram of ZVI/$H_2O_2$ removal of X-3B (pH 4.0, 8 mM $H_2O_2$, 50 mg $L^{-1}$ X-3B, 0.5 g $L^{-1}$ $Fe^0$, and $T$ = 25 °C).

reuse reaction was always higher than that after ZVI reused 1 time. And the removal rate of X-3B by ZVI/$H_2O_2$/WMF at 15 min also reached 85% during the 3rd and 4th reuse reactions. But the removal rate of X-3B by ZVI/$H_2O_2$/WMF at 15 min decreased to 34% during the 5th reuse test due to the serious loss of ZVI after 5 recycle reactions.

### Mechanism of WMF enhancing X-3B removal by ZVI/$H_2O_2$

The degradation of X-3B by ZVI/$H_2O_2$ system mainly depended on ·OH, and the methanol ($CH_3OH$) as the quencher of ·OH was added to the solution to further investigated the effect of ·OH on the system and confirmed the role of ·OH in the reaction process. As shown in Fig. 7, the removal rate of X-3B by ZVI/$H_2O_2$ decreased rapidly after methanol was added into the solution. In the presence of methanol with different concentrations, the removal of X-3B by ZVI/$H_2O_2$/WMF and ZVI/$H_2O_2$ was negligible. So ·OH could be considered as the main reactive oxidation species in ZVI/$H_2O_2$/WMF system, and the mechanism diagram was shown in Fig. 8.

In order to further investigate the effect of WMF on ZVI/$H_2O_2$ removal of X-3B, samples of UV-Vis were taken at different time during the reaction, and the scanning range was 200–800 nm. The decolorization of the dye was observed from the UV spectrum, and the degree of destruction of the molecular structure of the dye was analyzed. As shown in Fig. 9, X-3B had five characteristic absorption peaks. The absorption peaks at 538 nm and 512 nm in the visible region were caused by the conjugated structure of X-3B molecule, which made the dye unique red.[36] The absorption peaks at 330 nm, 284 nm, and 238 nm in the ultraviolet region correspond to the benzene ring and the naphthalene ring in the molecular structure of the dye.

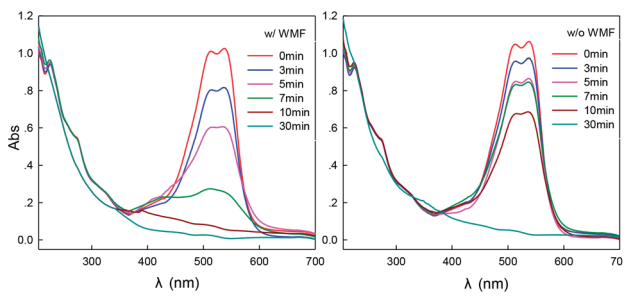


Fig. 9 UV-Vis absorption spectrum of ZVI removal of X-3B with or without WMF (pH 4.0, 8 mM $H_2O_2$, 50 mg $L^{-1}$ X-3B, 0.5 g $L^{-1}$ $Fe^0$, and $T$ = 25 °C).

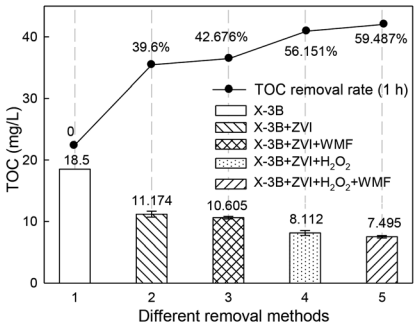


Fig. 10 TOC removal rate of X-3B under different removal methods (pH 4.0, 8 mM $H_2O_2$, 50 mg $L^{-1}$ X-3B, 0.5 g $L^{-1}$ $Fe^0$, and $T$ = 25 °C).

The azo bond in X-3B and the linked naphthalene ring and amino group are unstable, and the reaction is easily destroyed.[35] The two absorption peaks at 538 nm and 512 nm disappeared within 10 min in the presence of WMF which because of ·OH first attacked the azo bond of the dye, broke the conjugated system of X-3B. The absorption peaks at 238, 284 and 330 nm disappeared after 30 min, indicating that both the naphthalene rings and the triazinyl groups were destroyed and the dye had completely faded. The absorption peak only decreased within 30 min and the dye was not completely decolored in the absence of WMF. As shown in Fig. 10, the TOC removal rate of dye wastewater under different removal methods showed that the TOC removal rate of X-3B in the ZVI/$H_2O_2$/WMF system was as high as 59.49% in 1 h, which was significantly higher than that of ZVI, ZVI/WMF and ZVI/$H_2O_2$ systems. Obviously, the ZVI/$H_2O_2$/WMF system not only promoted the decolorization rate of X-3B, but also increased the degree of mineralization of X-3B wastewater.

The removal of X-3B by ZVI/$H_2O_2$ was a process in which ZVI was corroded as the main part, and could be described by eqn (1)–(3). ZVI was corroded, releasing $Fe^{2+}$ and $H_2O_2$ to react quickly to form ·OH to destroy the molecular structure of the dye and make it fade. Guan *et al.*[12] found that under aerobic conditions, $H_2O_2$ reacts with ZVI or $Fe^{2+}$ under acidic conditions. $Fe^{2+}$ could accelerate the Fenton reaction and allow a greater proportion of oxidants to be produced. When WMF was superimposed, the fading rate of dye molecules was accelerated, and the discoloration of X-3B mainly occurs in the first 10 min of WMF. The Lorentz force generated by the applied weak magnetic field and the magnetic field gradient force genera ted by the induced magnetic field generated on the surface of the ZVI act on $Fe^{2+}$, promoted the corrosion of ZVI, increased the release rate of $Fe^{2+}$, and generated more ·OH, promoted the dye molecules fade. WMF promoted the formation of $Fe^{2+}$ and accelerated the degradation rate of X-3B.

## Conclusions

On the basis of many experiments, the optimum conditions of Fenton-like reaction were obtained as follows: the concentration of reactive brilliant red X-3B was 50 mg $L^{-1}$, pH = 4.0, the dosage of ZVI with particle size of 20 μm was 0.5 g $L^{-1}$, and the dosage of $H_2O_2$ was 8 mM, the decolorization rate of X-3B could

 

reach 99.41% within 10 min. WMF extended the reaction pH range from 3.0 to 4.0. The initial main reaction process of removal of X-3B by ZVI/$H_2O_2$/WMF or ZVI/$H_2O_2$ was basically consistent with the zero-order reaction kinetics, but there was a large increased in the reaction rate when there was with WMF than when there was without WMF. The optimized magnetization time of ZVI pre-magnetization was 3 min. The effect of ZVI pre-magnetization was not as good as real-time magnetization, but ZVI pre-magnetization could shorten the magnetization time in the reaction process and reduce the reactor volume. ZVI reuse experiments clearly showed that the ZVI/$H_2O_2$/WMF system still had the ability to remove X-3B after 4 consecutive cycles, but the removal efficiency of ZVI would decrease. The decolorization of X-3B was mainly a hydroxyl radical attacked dye conjugate structure. Superimposed WMF greatly accelerated the degradation of X-3B by ZVI and shortens the reaction time. The WMF used in this study was produced by permanent magnets and did not require energy input. WMF applications were efficient, energy-efficient, free of harsh chemicals and environmental friendly, superimposed WMF to promote the removal of X-3B by ZVI/$H_2O_2$ was a promising and environmental friendly approach.

## Conflicts of interest

There are no conflicts to declare.

## Acknowledgements

The authors gratefully acknowledge the financial support of the National Natural Science Foundation of China (Grant No. 41807468), Zhejiang Provincial Natural Science Foundation of China (Grant No. LY18E080018), State Key Laboratory of Pollution Control and Resource Reuse Foundation, (Grant No. PCRRF18021).

## Notes and references

1 N. B. o. Statistics and M. o. E. Protection, *China Statistical yearbook on environment 2016*, Beijing, 2016.
2 L. Labiadh, A. Barbucci, G. Cerisola, A. Gadri, S. Ammar and M. Panizza, *J. Solid State Electrochem.*, 2015, **19**, 3177–3183.
3 K. Sathishkumar, M. S. AlSalhi, E. Sanganyado, S. Devanesan, A. Arulprakash and A. Rajasekar, *J. Photochem. Photobiol., B*, 2019, **200**, 111655.
4 A. J. dos Santos, I. Sirés, C. A. MartÃnez-Huitle and E. Brillas, *Chemosphere*, 2018, **210**, 1137–1144.
5 E. Brillas and C. A. Martínez-Huitle, *Appl. Catal., B*, 2015, **166**, 603–643.
6 M. M. Ghoneim, H. S. El-Desoky and N. M. Zidan, *Desalination*, 2011, **274**, 22–30.
7 E. Forgacs, T. Cserhati and G. Oros, *Environ. Int.*, 2004, **30**(1), 953–971.
8 C. Z. Liang, S. P. Sun, F. Y. Li, Y. K. Ong and T. S. Chung, *J. Membr. Sci.*, 2014, **469**, 306–315.
9 A. Y. Zahrim and N. Hilal, *Water Resour. Ind.*, 2014, **3**, 23–34.
10 Z. H. Huang, Y. Z. Li, W. J. Chen, J. H. Shi, N. Zhang, X. J. Wang, Z. Li, L. Z. Gao and Y. X. Zhang, *Mater. Chem. Phys.*, 2017, **202**, 266–276.
11 C. Grégorio, E. Lichtfous, L. D. Wilson and N. Morin-Crini, *Environ. Chem. Lett.*, 2018, 195–213.
12 X. H. Guan, Y. K. Sun, H. Qin, J. X. Li, I. M. C. Lo, D. He and H. R. Dong, *Water Res.*, 2015, **75**, 224–248.
13 J. S. Du, W. Q. Guo, D. Che and N. Ren, *Chem. Eng. J.*, 2018, **351**, 532–539.
14 L. J. Matheson and P. G. Tratnyek, *Environ. Sci. Technol.*, 1994, **28**, 2045–2053.
15 Y. H. Liou, S. L. Lo, C. J. Lin, W. H. Kuan and S. C. Weng, *J. Hazard. Mater.*, 2005, **126**, 189–194.
16 C. B. Wang and W. X. Zhang, *Environ. Sci. Technol.*, 1997, **31**, 2154–2156.
17 S. Harendra and C. Vipulanandan, *Colloids Surf., A*, 2008, **322**, 6–13.
18 C. Lee, J. Y. Kim, W. I. Lee, K. L. Nelson, J. Yoon and D. L. Sedlak, *Environ. Sci. Technol.*, 2008, **42**, 4927–4933.
19 L. J. Zhou, W. Q. Zhuang, X. Wang, K. Yu, S. F. Yang and S. Q. Xia, *Water Res.*, 2017, **111**, 140–146.
20 D. H. Phillips, B. Gu and D. B. Watson, *Environ. Sci. Technol.*, 2000, **34**, 4169–4176.
21 Y. Roh, S. Y. Lee and M. P. Elless, *Environ. Geol.*, 2000, **40**, 184–194.
22 L. P. Liang, X. H. Guan, Z. Shi, J. L. Li, Y. Wu and P. G. Tratnyek, *Environ. Sci. Technol.*, 2014, **48**, 6326–6334.
23 J. X. Li, H. J. Qin, W. X. Zhang, Z. Shi, D. Y. Zhao and X. H. Guan, *Sep. Purif. Technol.*, 2017, **176**, 40–47.
24 L. P. Liang, W. Sun, X. H. Guan, Y. Y. Huang, W. Choi, H. L. Bao, L. Li and Z. Jiang, *Water Res.*, 2014, **49**, 371–380.
25 H. Y. Xu, Y. K. Sun, J. X. Li, F. M. Li and X. H. Guan, *Environ. Sci. Technol.*, 2016, **50**, 8214–8222.
26 J. X. Li, H. J. Qin and X. H. Guan, *Environ. Sci. Technol.*, 2015, **49**, 14401–14408.
27 Y. K. Sun, Y. H. Hu, T. L. Huang, J. X. Li and X. H. Guan, *Environ. Sci. Technol.*, 2017, **51**, 3742–3750.
28 X. M. Xiong, Y. K. Sun, B. Sun, W. H. Song, J. Y. Sun, N. Y. Gao, J. L. Qiao and X. H. Guan, *RSC Adv.*, 2015, **5**, 13357–13365.
29 X. M. Xiong, B. Sun, J. Zhang, N. Y. Gao, J. M. Shen, J. L. Li and X. H. Guan, *Water Res.*, 2014, **62**, 53–62.
30 X. Li, M. H. Zhou, Y. W. Pan and L. T. Xu, *Chem. Eng. J.*, 2017, **307**, 1092–1104.
31 Y. W. Pan, M. H. Zhou, X. Li, L. T. Xu, Z. X. Tang, X. J. Sheng and B. Li, *Chem. Eng. J.*, 2017, **318**, 50–56.
32 X. Li, M. H. Zhou, Y. W. Pan, L. T. Xu and Z. X. Tang, *Sep. Purif. Technol.*, 2017, **178**, 49–55.
33 Y. W. Pan, M. H. Zhou, X. Li, L. T. Xu, Z. X. Tang and M. M. Liu, *Sep. Purif. Technol.*, 2016, **169**, 83–92.
34 A. Ghauch, H. Baydoun and P. Dermesropian, *Chem. Eng. J.*, 2011, **172**, 18–27.
35 A. Goi and M. Trapido, *Chemosphere*, 2002, **46**, 913–922.
36 Y. P. Mao, Y. Tao, Z. M. Shen, Y. M. Lei and W. H. Wang, *Environ. Sci. Technol.*, 2009, **32**(19), 67–70.